Published for SISSA by Springer

Received: May 8, 2015
Accepted: June 10, 2015
Published: July 1, 2015

# $\mathcal{O}(1)$ GeV dark matter in SUSY and a very light pseudoscalar at the LHC

**Chengcheng Han,**[a] **Doyoun Kim,**[a] **Shoaib Munir**[a] **and Myeonghun Park**[a,b,c]

[a] *Asia Pacific Center for Theoretical Physics, San 31, Hyoja-dong, Nam-gu, Pohang 790-784, Republic of Korea*
[b] *Department of Physics, Postech, Pohang 790-784, Korea*
[c] *Kavli IPMU (WPI), The University of Tokyo, Kashiwa, Chiba 277-8583, Japan*

*E-mail:* hancheng@apctp.org, doyoun.kim@apctp.org, s.munir@apctp.org, parc@apctp.org

Abstract: We analyze the prospects of the detection of an $\mathcal{O}(1)$ GeV neutralino dark matter, $\widetilde{\chi}_1^0$, in the Next-to-Minimal Supersymmetric Standard Model at the 14 TeV LHC. We perform dedicated scans of the relevant parameter space of the model and find a large number of points where the thermal relic abundance due to such a dark matter is consistent with the PLANCK measurement. We note that this dark matter is highly singlino-dominated and is always accompanied by a pseudoscalar, $A_1$, with a mass around twice its own, which is responsible for its resonant annihilation. For two benchmark points from our scan, we then carry out a detector-level signal-to-background analysis of the pair production of a heavier higgsino neutralino and a chargino. The higgsino thus produced decays into the dark matter and either the $Z$ boson or the $A_1$. For the $Z$-associated production of $\widetilde{\chi}_1^0$, we investigate the scope of the trilepton search channel. For the $A_1$-associated production mode, in order to identify the two collimated muons coming from the decay of the $A_1$, we employ an unconventional method, of clustering them together into one jet-like object. Using this method, for certain parameter space configurations, a much larger sensitivity can be obtained at the 14 TeV LHC for the $A_1\widetilde{\chi}_1^0$ channel compared to the $Z\widetilde{\chi}_1^0$ channel, with an integrated luminosity of 300 fb$^{-1}$.

Keywords: Supersymmetry Phenomenology

ArXiv ePrint: 1504.05085



doi:10.1007/JHEP07(2015)002

JHEP07(2015)002

## Contents



JHEP07(2015)002

## 1 Introduction

The Minimal Supersymmetric Standard Model (MSSM) contains three neutral Higgs states. The lightest one of these, $h$, is one of the main candidates for the Higgs boson, $H_{\rm obs}$, observed at the Large Hadron Collider (LHC) [1, 2]. The MSSM also contains a total of four neutralino mass eigenstates, the lightest of which, $\widetilde{\chi}_1^0$, is an important dark matter (DM) candidate, when it is also the lightest supersymmetric particle (LSP) and $R$-parity is conserved. Despite its being a theoretically sound and highly predictive model, the absence of any evidence of supersymmetry (SUSY) during Run-I of the LHC has brought the MSSM under increased scrutiny recently. This is because the only way for $h$ to gain a mass close to the one measured for the $H_{\rm obs}$ is through large radiative corrections from the SUSY sector. The most dominant of these corrections come from the stops, which warrants either TeV-scale SUSY-breaking masses for them or a multi-TeV stop mixing parameter, $A_t$. This in turn leads to excessive fine-tuning of the model parameters such as the soft masses of the two Higgs doublet fields, $H_u$ and $H_d$, and the Higgs-higgsino mass paramater $\mu$, given the measured mass of the $Z$ boson.

The parameters of the MSSM get further constrained if one requires, in addition to $h$ fulfilling the role of the observed Higgs boson, $\widetilde{\chi}_1^0$ to generate the observed *thermal* DM relic density of the universe, $\Omega_{\rm DM}$, as measured by the WMAP [3] and PLANCK [4] telescopes. This condition is strongly dependent on the interplay between the mass and the composition of the $\widetilde{\chi}_1^0$, as these quantities govern its annihilation rate into pairs of SM particles. The $\widetilde{\chi}_1^0$ is a pure higgsino when $M_1$, $M_2 \gg \mu$, with $M_1$ and $M_2$ being the soft gaugino masses, and can only yield the correct relic abundance if $\mu \sim 1\,\text{TeV}$. If $\widetilde{\chi}_1^0$ is instead a bino-higgsino mixture, it can give sufficient $\Omega_{\rm DM}$ for comparatively smaller masses, by annihilating via chargino/neutralino exchanges into pairs of vector bosons. A predominantly bino-like $\widetilde{\chi}_1^0$,

on the other hand, can be consistent with the measured $\Omega_{\rm DM}$ for much smaller masses, provided one of the third-generation sfermions is not much heavier than itself. In fact, if such a $\widetilde{\chi}_1^0$ has a mass $\lesssim 65\,\text{GeV}$, it can undergo annihilation via $h$ in the $s$-channel into a $b\bar{b}$ pair (see, e.g., [5, 6]). For even smaller bino masses, the right amount of $s$-channel annihilation can occur through the $Z$ boson. Evidently, the cross section for annihilation via $h$ or $Z$ falls abruptly as the difference between $m_{\widetilde{\chi}_1^0}$ and $m_h/2$ or $m_Z/2$, respectively, increases. Below $m_{\widetilde{\chi}_1^0} \lesssim 30\,\text{GeV}$ it is thus generally impossible to obtain sufficient $\Omega_{\rm DM}$ in the MSSM due to the absence of a mediator with the correct mass.

The Next-to-Minimal Supersymmetric Standard Model (NMSSM) [7–10] contains a gauge singlet Higgs superfield, $\widehat{S}$, in addition to the two doublet superfields, $\widehat{H}_d$ and $\widehat{H}_u$, of the MSSM. This results in two additional neutral mass eigenstates in the Higgs sector besides the three similar to the MSSM ones. Thus, in total there are seven Higgs bosons in the NMSSM; CP-even $H_{1,2,3}$, CP-odd $A_{1,2}$ and a charged pair, $H^\pm$. Naturally, the two new Higgs bosons are dominated by the scalar component of $\widehat{S}$, which implies that their couplings to the fermions and gauge bosons of the Standard Model (SM) are typically much smaller than those of the doublet-like Higgs bosons. Their masses are thus generally very weakly constrained by the Higgs boson data from the Large Electron Positron (LEP) collider, the Tevatron or the LHC, and can be as low as a GeV or so. Similarly, the neutralino sector of the NMSSM also contains five mass eignestates, one more than in the MSSM. The fifth neutralino is dominated by the fermion component of $\widehat{S}$, commonly referred to as the singlino.

In the NMSSM, the role of the $H_{\rm obs}$ can be played by either one of the $H_1$ and $H_2$ [11–15] or even by a combination/superposition of these two when both of them lie near 125 GeV [16–18]. Evidently, when $H_{\rm obs}$ is the $H_1$, only $A_1$ can be lighter than it. Conversely, when $H_{\rm obs}$ is the $H_2$, there exist the possibilities of either the $H_1$ alone or both the $H_1$ and $A_1$ being lighter than it. Such light $H_1$ or $A_1$ can act as mediators for the annihilation of a $\widetilde{\chi}_1^0$ as light as a GeV or so in order for it to generate the correct $\Omega_{\rm DM}$ — a scenario precluded in the MSSM. Note that the electroweak (EW) baryogenesis may also be accommodated within this framework when the $\widetilde{\chi}_1^0$ mass is below 10 GeV [19, 20]. Additionally, a light NMSSM $\widetilde{\chi}_1^0$ can explain the galactic centre $\gamma$-ray excess [21, 22] observed by the Fermi Large Area Telesope in the presence of a light $A_1$ [20, 23–25].[1] If the $\widetilde{\chi}_1^0$ is even lighter, it has been shown [26, 27] to explain the CDMS-II event excess near 10 GeV [28]. However, further experimental evidence is necessary to confirm whether any of these events are indeed caused by the annihilation of the DM and the jury is still out on its correct mass. While the direct-detection experiments such as DAMA/LIBRA [29], CoGeNT [30, 31], CRESST-II [32], XENON100 [33] and LUX [34] can cover a wide range of the DM mass, it is extremely unlikely for them to reach below $\sim 2\,\text{GeV}$ [35]. Similarly, while the IceCube neutrino observatory also shows some promise [36] for the indirect detection of the NMSSM DM, the sensitivity for a mass below 10 GeV is very poor.

[1] In the case of an $H_1$, the $s$-channel annihilation is $p$-wave suppressed and hence generally negligible. Furthermore, due to the strong correlation between the masses of $H_1$ and $H_2$, as will be shown later, it is very difficult, although possible, to obtain an $H_1$ as light as a GeV or so while requiring $H_2$ to have a mass near 125 GeV.



JHEP07(2015)002

The Run-II of LHC can prove very crucial in this regard, owing to its potential to probe a very light DM, produced in association with the $Z$ boson or the $A_1$ in the decays of the heavier neutralinos. In some recent studies [37–41] it has been shown that significant regions of the NMSSM parameter space can be covered by the $Z$-associated production of the $\widetilde{\chi}_1^0$ at the LHC Run-II, with the $Z$ decaying into two leptons. The $\widetilde{\chi}_{2,3}^0 \to A_1 + \widetilde{\chi}_1^0$ channel has also shown some promise [42] even for the 8 TeV LHC, with the mass of the $A_1$ lying above the $\tau^+\tau^-$ production threshold. These search channels can be complemented by those where the light $A_1$ is not accompanied by the DM. As long as the relic abundance is satisfied for a given SUSY point with a very light DM, observation of the corresponding $A_1$, which would be a likely mediator for its annihilation, could serve as a pointer. Such channels include, most importantly, decays of the $H_{\rm obs}$ into $A_1 + A_1$ or $A_1 + Z$ [43–49]. At the Run-I of LHC, light pseudoscalars decaying in the $\mu^+\mu^-$ channel have already been probed, when they are produced either singly in $pp$ collisions [50] or in pairs from the decays of a 125 GeV Higgs boson [51]. These searches thus strongly constrain the parameter space of the NMSSM. Prospects for the observability of $A_1$ at the 14 TeV LHC have been analyzed in detail recently in [52–54], with the measurement of the mass of $H_{\rm obs}$ providing an additional handle in the kinematic selection of the events. The channels investigated in all these analyses, however, show sufficient sensitivity only for an $A_1$ heavier than 5 GeV.

In this study we focus on the production of a very light, $\mathcal{O}(1)$ GeV, $\widetilde{\chi}_1^0$ via decays of the heavier, higgsino-like, neutralinos of the NMSSM. We perform detailed scans of the NMSSM parameter space to highlight its regions where such a $\widetilde{\chi}_1^0$, consistent with the observed relic abundance of the universe, can be obtained in the presence of a SM-like $H_2$. We discuss some important characteristics of these parameter regions and of the $\widetilde{\chi}_1^0$. We note, in particular, that the $\widetilde{\chi}_1^0$ is always accompanied by a pseudoscalar with a mass nearly twice its own. We then carry out comprehensive detector-level analyses of the $Z$- as well as $A_1$-associated productions of the $\widetilde{\chi}_1^0$. For the $A_1 + \widetilde{\chi}_1^0$ production channel, we adopt an unconventional method for reconstructing the pair of highly collinear muons that result from the subsequent decay of the $A_1$. We find that by using our signal reconstruction method the $A_1 + \widetilde{\chi}_1^0$ channel can have a better signal strength at the 14 TeV LHC compared to the $Z + \widetilde{\chi}_1^0$ channel for certain specific parameter configurations. Therefore, the $A_1 + \widetilde{\chi}_1^0$ channel can serve as a crucial probe of new physics, complementing well the $Z + \widetilde{\chi}_1^0$ channel for very a low-mass singlino-dominated DM.

The article is organized as follows. In section 2, we will briefly discuss the NMSSM and its singlet sector. In section 3 we will present some details of our findings from the numerical scans of the NMSSM parameter space. In section 4 we will explain our signal-to-background analyses and in section 5 we will show their results. We will present our conclusions in section 6.

## 2 The singlet sector of the NMSSM

The scale-invariant superpotential of the NMSSM (see, e.g., [55, 56] for reviews) is written as

$$W_{\rm NMSSM} = \text{MSSM Yukawa terms} \; + \; \lambda \widehat{S} \widehat{H}_u \widehat{H}_d \; + \; \frac{\kappa}{3} \, \widehat{S}^3 \,, \tag{2.1}$$



JHEP07(2015)002

where $\lambda$ and $\kappa$ are dimensionless Yukawa couplings. The above superpotential observes a discrete $Z_3$ symmetry, which forbids the $\mu\widehat{H}_u\widehat{H}_d$ term present in the MSSM superpotential and at the same time breaks the dangerous Peccei-Quinn (PQ) symmetry [57, 58]. Here, an effective $\mu$-term is generated upon spontaneous symmetry breaking, when $\widehat{S}$ develops a vacuum expectation value (VEV), $s \equiv \langle\widehat{S}\rangle$, so that $\mu_{\rm eff} = \lambda s$. The soft SUSY-breaking terms in the scalar Higgs sector are then given by

$$V_{\rm soft} = m_{H_u}^2|H_u|^2 + m_{H_d}^2|H_d|^2 + m_S^2|S|^2 + \left(\lambda A_\lambda S H_u H_d + \frac{1}{3}\kappa A_\kappa S^3 + \text{h.c.}\right) . \tag{2.2}$$

Through the minimization conditions of the complete tree-level Higgs potential, the soft masses $m_{H_u}$, $m_{H_d}$ and $m_S$ can be traded for the respective VEVs, $v_u$, $v_d$ and $s$, of the corresponding Higgs fields.

The neutral scalar and pseudoscalar Higgs mass matrices are obtained from the Higgs potential evaluated at the vacuum. Diagonalization of these matrices yields the mass expressions for the five neutral Higgs bosons. The tree-level masses of the two lightest CP-even Higgs bosons, which are of our interest here, can be approximated, for moderate-to-large $\tan\beta$ ($\equiv v_u/v_d$) and EW-scale dimensionful parameters, by [59]

$$m_{H_{1,2}}^2 \approx \frac{1}{2}\left\{m_Z^2 + 4(\kappa s)^2 + \kappa s A_\kappa \mp \sqrt{\left[m_Z^2 - 4(\kappa s)^2 - \kappa s A_\kappa\right]^2 + 4\lambda^2 v^2\left[2\lambda s - (A_\lambda + \kappa s)\sin 2\beta\right]^2}\right\} , \tag{2.3}$$

where $v \equiv \sqrt{v_u^2 + v_d^2} \simeq 174\,\text{GeV}$. Thus there is a strong correlation between the masses of $H_1$ and $H_2$, implying that requiring one of these to lie near 125 GeV constrains the other also. Similarly, the tree-level mass of the singlet-like pseudoscalar can be given, assuming negligible singlet-doublet mixing, by the approximate expression

$$m_{A_1}^2 \simeq \lambda(A_\lambda + 4\kappa s)\frac{v^2 \sin 2\beta}{2s} - 3\kappa s A_\kappa \, . \tag{2.4}$$

The neutralino mass matrix in the NMSSM is written as

$$\mathcal{M}_{\widetilde{\chi}^0} = \begin{pmatrix} M_1 & 0 & -m_W \tan\theta_W \cos\beta & m_W \tan\theta_W \sin\beta & 0 \\ 0 & M_2 & m_W \cos\beta & -m_W \sin\beta & 0 \\ -m_W \tan\theta_W \cos\beta & m_W \cos\beta & 0 & -\mu_{\rm eff} & -\lambda v_u \\ m_W \tan\theta_W \sin\beta & -m_W \sin\beta & -\mu_{\rm eff} & 0 & -\lambda v_d \\ 0 & 0 & -\lambda v_u & -\lambda v_d & 2\kappa s \end{pmatrix} , \tag{2.5}$$

with $m_W$ being the mass of the $W$ boson and $\theta_W$ being the weak mixing angle. This symmetric mass matrix can be diagonalized by a unitary matrix $N$ to obtain the five neutralino states, $\widetilde{\chi}_{1-5}^0$, ordered by their masses, implying that the $\widetilde{\chi}_1^0$ is the LSP. This mass eigenstate is given by the linear combination

$$\widetilde{\chi}_1^0 = N_{11}\widetilde{B}^0 + N_{12}\widetilde{W}_3^0 + N_{13}\widetilde{H}_d^0 + N_{14}\widetilde{H}_u^0 + N_{15}\widetilde{S}^0. \tag{2.6}$$

We define the gaugino fraction in $\widetilde{\chi}_1^0$ as $Z_g = |N_{11}|^2 + |N_{12}|^2$, the higgsino fraction as $Z_h = |N_{13}|^2 + |N_{14}|^2$ and the singlino fraction as $Z_s = |N_{15}|^2$. The composition of $\widetilde{\chi}_1^0$ thus depends on the values of the various model parameters appearing in the above mass matrix.



JHEP07(2015)002

In the MSSM, the fifth row and column, corresponding to the singlino and hence containing the $\lambda$-dependent terms, do not exist. There, the smaller the $\mu$ compared to the $\min[M_1, M_2]$, the larger the higgsino fraction in $\widetilde{\chi}_1^0$. Since the mass of the higgsino-like chargino, which is the lighter $\widetilde{\chi}_1^\pm$ in this case, is also proportional to $\mu$, the value of this parameter is bounded from below to around 100 GeV by the non-observation of a chargino at the large electron positron (LEP) collider. On the other hand, in order to avoid excessive fine-tuning of the model parameters for obtaining the correct Higgs boson mass, $\mu$ ought not to be too large. However, a purely higgsino LSP does not give the correct thermal relic density for masses below $\sim 1$ TeV, as the annihilation cross section becomes too large. Therefore, the only way for the $\widetilde{\chi}_1^0$ in the MSSM to give good relic abundance with a mass $\mathcal{O}(10)$ GeV is to have a sizable bino component [6, 60].

In the NMSSM, the presence of the singlino leads to some additional possibilities in the context of DM phenomenology. In the limit $\mu_{\rm eff} \ll \min[M_1, M_2]$, the term $[\mathcal{M}_{\widetilde{\chi}^0}]_{55} = 2\kappa s = 2\frac{\kappa\mu_{\rm eff}}{\lambda}$ in eq. (2.5) implies that the LSP is singlino-dominated for $2\kappa/\lambda < 1$. The singlino fraction in $\widetilde{\chi}_1^0$ can be increased by reducing $\kappa$. One could alternatively increase $\lambda$, while keeping $\mu_{\rm eff}$ fixed, to reduce the size of the $[\mathcal{M}_{\widetilde{\chi}^0}]_{55}$ term, but this also enlarges the sizes of the off-diagonal mixing terms. Eq. (2.4) shows that the mass of $A_1$ also scales with $\kappa s$. Thus a light singlino-like $\widetilde{\chi}_1^0$ can be naturally accompanied by a light $A_1$. Note that the strong correlation, eq. (2.3), between the $H_2$ mass, which is required to be around 125 GeV, and the $H_1$ mass generally prevents the latter from taking very low values, although it also scales mainly with $\kappa s$. Importantly though, even if $H_1$ has a mass close to $2\widetilde{\chi}_1^0$, the $\widetilde{\chi}_1^0$ annihilation via $s$-channel $H_1$ is $p$-wave suppressed, which would make it extremely difficult to generate the correct thermal relic abundance. We therefore focus only on a light $A_1$ here, which can result in the singlino-like $\widetilde{\chi}_1^0$ yielding the correct relic density even with its mass around a GeV.

As noted in the Introduction, the light $\widetilde{\chi}_1^0$ can be produced in the decays of the heavier neutralinos. In particular, the $\widetilde{\chi}_2^0$ and $\widetilde{\chi}_3^0$ as well as the $\widetilde{\chi}_1^\pm$ in this scenario with a light singlino-like DM are predominantly higgsinos [42]. Their main production channel is $pp \to \widetilde{\chi}_{2,3}^0 + \widetilde{\chi}_1^\pm$, which is followed by the decays $\widetilde{\chi}_{2,3}^0 \to Z/A_1 + \widetilde{\chi}_1^0 \to \ell^+\ell^- + \not{E}_T$ and $\widetilde{\chi}_1^\pm \to W^\pm + \widetilde{\chi}_1^0 \to \ell^\pm + \not{E}_T$, where $\not{E}_T$ implies missing transverse energy. The complete processes are shown in figure 1, (a) and (b). The $Z + \widetilde{\chi}_1^0$ decay channel of the $\widetilde{\chi}_{2,3}^0$ is by far the dominant one, while $\widetilde{\chi}_{2,3}^0 \to A_1 + \widetilde{\chi}_1^0$ is generally suppressed. The $Z + W + \not{E}_T$ production, which results in trileptonic final states, is therefore the preferred search channel for the higgsinos, also since it has minimal dependence on $m_{\widetilde{\chi}_1^0}$. Dedicated searches carried out by both the CMS and ATLAS collaborations [61–63] have either already put strong constraints on significant regions of the NMSSM parameter space or are likely to cover large portions of it, where the $\widetilde{\chi}_1^0$ can be as light as a GeV, at the LHC Run-II.

It is, however, important to note that, for sufficiently large values of the parameter $\lambda$, the branching ratio (BR) for the $\widetilde{\chi}_{2,3}^0 \to A_1 + \widetilde{\chi}_1^0$ decay channel, while still subdominant, can become sizable. For $A_1$ masses of interest here, i.e., below the $\tau^+\tau^-$ threshold, the decay mode with the largest BR is $A_1 \to c\bar{c}$. The main leptonic decay channel, $A_1 \to \mu^+\mu^-$, is highly subdominant, with its BR never exceeding 9%, as we shall see below. This value is still larger than twice that of the BR($Z \to \mu^+\mu^-$) ($\simeq 0.034$). But one challenge that arises



JHEP07(2015)002

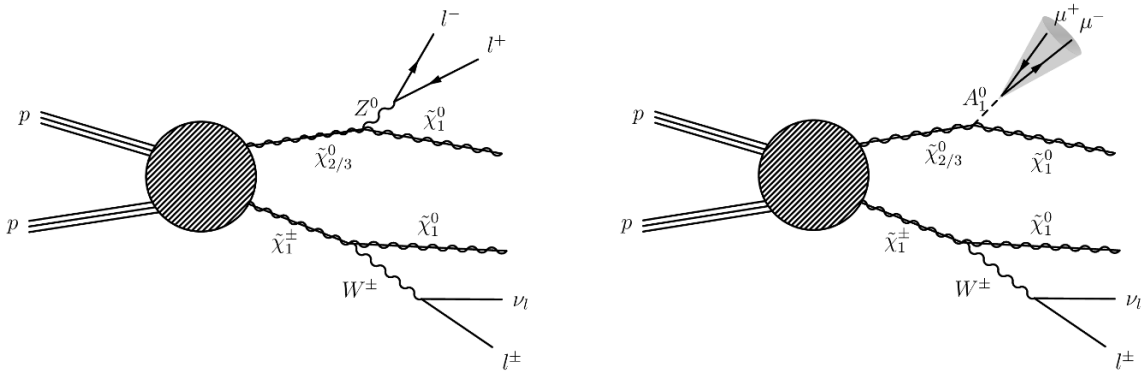


**(a)** **(b)**

**Figure 1.** Production process for the $\widetilde{\chi}_{2,3}^0\widetilde{\chi}_1^\pm$ pair, with the $\widetilde{\chi}_{2,3}^0$ decaying via (a) $Z + \widetilde{\chi}_1^0$ and (b) $A_1 + \widetilde{\chi}_1^0$.

in this context is the reconstruction of the very light $A_1$ from two highly collinear muons it decays into and the isolation of this signal from the background. As long as this complication can be overcome, the two observations above imply that the $A_1+\widetilde{\chi}_1^0$ search channel can possibly complement the $Z\widetilde{\chi}_1^0$ channel for certain specific NMSSM parameter space points. In the following sections we will analyze such parameter combinations and also introduce our method for reconstructing the very light $A_1$ from two collinear muons. We should point out here that while in principle the same method can alternatively be used to probe these $A_1$'s in the decays of the heavy CP-even Higgses, our requirement of the presence of $\not{E}_T$ in the final state, as an indication of light DM, renders these channels irrelevant here.

## 3 Parameter space scan and constraints

Due to the presence of the additional singlet superfield, the NMSSM contains several new parameters besides the 115 or so of the MSSM at the EW scale. However, assuming the sfermion mass matrices and the scalar trilinear coupling matrices to be diagonal reduces the parameter space of the model considerably. In this study, since our main focus is the higgsino-singlino sector, we further assume the following universality conditions.

$$\begin{aligned} M_0 &\equiv M_{Q_{1,2,3}} = M_{U_{1,2,3}} = M_{D_{1,2,3}} = M_{L_{1,2,3}} = M_{E_{1,2,3}}\,, \\ M_{1/2} &\equiv 2M_1 = M_2 = \frac{1}{3}M_3\,, \\ A_0 &\equiv A_t = A_b = A_\tau\,, \end{aligned} \tag{3.1}$$

where $M_{Q_{1,2,3}}$, $M_{U_{1,2,3}}$, $M_{D_{1,2,3}}$, $M_{L_{1,2,3}}$ and $M_{E_{1,2,3}}$ are the soft masses of the sfermions, $M_{1,2,3}$ those of the gauginos and $A_{t,b,\tau}$ the trilinear Higgs-sfermion couplings. Along with $M_0$, $M_{1/2}$ and $A_0$, the model then contains $\lambda$, $\kappa$, $\mu_{\rm eff}$, $\tan\beta$, $A_\lambda$ and $A_\kappa$ as the only free parameters, which are input at the SUSY-breaking scale, $M_{\rm SUSY} = \sqrt{m_{\tilde{t}_1} m_{\tilde{t}_2}}$, with $m_{\tilde{t}_{1,2}}$ being the physical masses of the two stops.



JHEP07(2015)002

| Parameter | Scanned range |
|---|---|
| $M_0$ (GeV) | 500–2000 |
| $M_{1/2}$ (GeV) | 300–1000 |
| $A_0$ (GeV) | 0–4000 |
| $\mu_{\rm eff}$ (GeV) | 100–300 |
| $\tan\beta$ | 6–25 |
| $\lambda$ | 0.01–0.4 |
| $\kappa$ | $10^{-5}$–$10^{-1}$ |
| $A_\lambda$ (GeV) | 0–5000 |
| $A_\kappa$ (GeV) | −100–0 |

**Table 1.** Ranges of the NMSSM input parameters scanned for obtaining $\widetilde{\chi}_1^0$ with a mass below 2 GeV.

We performed a scan of the above mentioned nine parameters using the nested sampling package MultiNest-v2.18 [64], which was interfaced with NMSSMTools-v4.5.0 [65–68] for calculation of the SUSY mass spectrum and BRs for each model point sampled. The scanned ranges of the parameters are given in table 1 and were chosen, based loosely on the findings of [42], to maximally yield points with $m_{\widetilde{\chi}_1^0} \lesssim 2\,\text{GeV}$ as well as the $H_2$ having a mass near the one measured for the $H_{\rm obs}$ at the LHC. The $H_2$ was additionally required to have SM-like signal rates. The signal rate, obtained from NMSSMTools as an output, is defined, for a given decay channel $X$, as

$$R^X \equiv \frac{\sigma(gg \to H_2) \times \text{BR}(H_2 \to X)}{\sigma(gg \to h_{\rm SM}) \times \text{BR}(h_{\rm SM} \to X)}\,, \tag{3.2}$$

where $h_{\rm SM}$ is the SM Higgs boson with a mass equal to $m_{H_2}$.

A very light $A_1$ is subject to constraints from direct collider searches as well as from flavor physics [69]. The program NMSSMTools intrinsically takes into account the exclusion limits on pseudoscalars from LEP and BaBar as well as from the $4\mu$ searches at the CMS [51]. Additionally, It ensures that the LEP limit on the $\widetilde{\chi}_1^\pm$ mass and the perturbativity constraints on the various Higgs boson couplings are satisfied and that the $\widetilde{\chi}_1^0$ is the LSP. We further required each scanned point to satisfy the following constraints:

- $2.63 \times 10^{-4} \leq \text{BR}\left(\overline{\text{B}} \to \text{X}_\text{s}\gamma\right) \leq 4.23 \times 10^{-4}$,
- $0.71 \times 10^{-4} \leq \text{BR}\left(\text{B}_\text{u} \to \tau\nu\right) \leq 2.57 \times 10^{-4}$,
- $1.3 \times 10^{-9} \leq \text{BR}\left(\text{B}_\text{s} \to \mu^+\mu^-\right) \leq 4.5 \times 10^{-9}$,
- $0.107 \leq \Omega_{\widetilde{\chi}_1^0} h^2 \leq 0.131$,
- $122\,\text{GeV} \leq m_{H_2} \leq 128\,\text{GeV}$.



JHEP07(2015)002

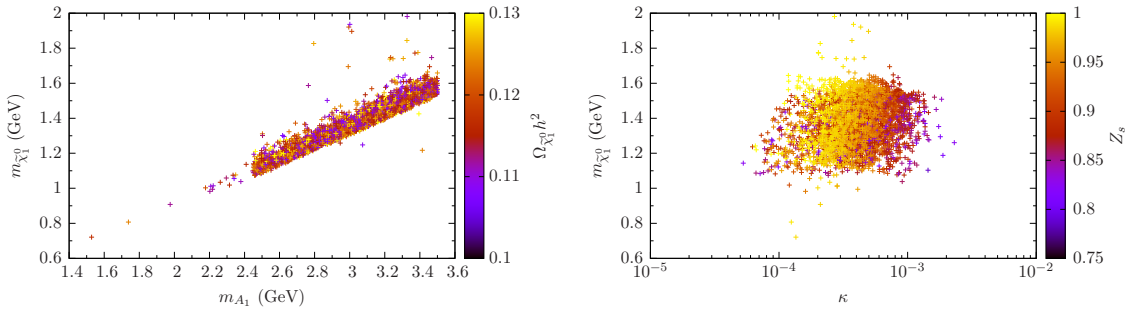


**(a)** **(b)**

**Figure 2.** (a) The distribution of the $\widetilde{\chi}_1^0$ mass vs. that of the $A_1$ mass, with the heat map corresponding to the relic abundance. (b) The dependence of $m_{\widetilde{\chi}_1^0}$ on the parameter $\kappa$. The heat map shows the singlino fraction in the $\widetilde{\chi}_1^0$.

The $b$-physics observables above were calculated using the package SuperIso-v3.4 [70] and the relic density using the MicrOMEGAs-v4.1.5 [71] package. The allowed range of $\Omega_{\widetilde{\chi}_1^0}$ assumes a $\pm 10\%$ theoretical error around the central value of 0.119 measured by the PLANCK telescope [4]. Similarly an error of $\pm 3$ GeV is allowed in the theoretical estimation of the $H_2$ mass, given the $H_{\rm obs}$ mass measurement of 125 GeV at the LHC. Consistency with the LEP and LHC exclusion limits on the non-SM-like Higgs bosons, including the $A_1$, was further ensured by testing each point that passed the above constraints with the program HiggsBounds-v4.2.0 [72–75].

In figure 2(a) we show the ranges of the $A_1$ and $\widetilde{\chi}_1^0$ masses obtained for the good points from our scan. The heat map corresponds to the $\widetilde{\chi}_1^0$ relic density. One can see a strong correlation between $m_{\widetilde{\chi}_1^0}$ and $m_{A_1}$, with the former almost always being half of the latter in order for the resonant annihilation of the $\widetilde{\chi}_1^0$ via the $A_1$. The tiny $\widetilde{\chi}_1^0$ masses are a result of vanishing $\kappa$ as seen in figure 2(b), implying an almost PQ-symmetric model. The heat map in the figure shows the distribution of the singlino fraction in the $\widetilde{\chi}_1^0$ which increases as $\kappa$ decreases and is always larger than 0.75. A large singlino component implies a small higgsino fraction, which is necessary to prevent an under abundance of the $\widetilde{\chi}_1^0$ from too much annihilation. Figure 3(a) illustrates that the $A_1$ is restricted to a lower mass, needed for satisfying the relic density constraint, by adjusting $A_\kappa$ to a narrow range of low negative values. This is in agreement with eq. (2.4), along with the fact that $\lambda$, illustrated by the heat map in the figure, also generally tends to be small. In figure 3(b) the distributions of the parameters $A_\lambda$ and $\mu_{\rm eff}$ are shown against the $H_1$ mass range obtained in the scan. We see that when both $A_\lambda$ and $\tan\beta$ are small $m_{H_1}$ is low, while its maximum value, $\sim 45$ GeV, is obtained for the largest allowed values of $A_\lambda$, with $\tan\beta \gtrsim 10$.

Figure 4(a) shows that the mass of the $\widetilde{\chi}_2^0$ is almost equal to the parameter $\mu_{\rm eff}$ as long the parameter $M_{1/2}$, given by the color map, approaches its maximum allowed value. As the splitting between $M_{1/2}$ and $\mu_{\rm eff}$ decreases, the gaugino-higgsino mixing increases,



JHEP07(2015)002

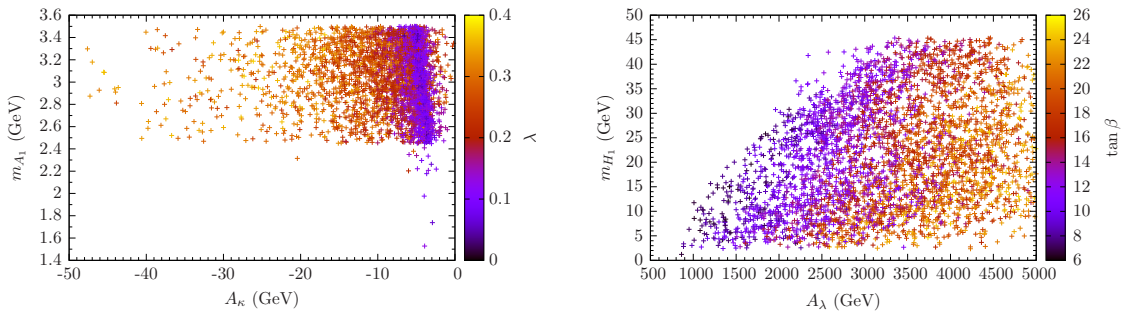


**(a)** **(b)**

**Figure 3.** (a) The mass of $A_1$ as a function of the parameters $A_\kappa$ and $\lambda$. (b) The mass of $H_1$ vs. the distributions of the parameters $A_\lambda$ and $\tan\beta$.

which results in somewhat lowering $m_{\widetilde{\chi}^0_2}$ relative to $\mu_{\rm eff}$. Figure 4(b) similarly shows that, since the $\widetilde{\chi}^0_3$ and the $\widetilde{\chi}^\pm_1$ are higgsino-like as well, their masses are also proportional to $\mu_{\rm eff}$. Moreover, the $\widetilde{\chi}^\pm_1$ is always almost mass-degenerate with $\widetilde{\chi}^0_2$, while $\widetilde{\chi}^0_3$ is generally heavier than both of them, but only slightly so.[2] Figure 5(a) illustrates that the BR($\widetilde{\chi}^0_2 \to A_1\widetilde{\chi}^0_1$) increases with $\lambda$, shown by the heat map. This is because, for vanishing singlet-doublet mixing in the pseudoscalar mass matrix as well as singlino-higgsino mixing in the neutralino mass matrix, the coupling between the $A_1$, $\widetilde{\chi}^0_1$ and $\widetilde{\chi}^0_2$, given by eq. (A.14) of [55], can be approximated by the simple relation

$$g_{A_1\widetilde{\chi}^0_1\widetilde{\chi}^0_2} \approx -\frac{i}{20}(\lambda - 2\sqrt{2}\kappa)\,. \tag{3.3}$$

Still, the BR($\widetilde{\chi}^0_2 \to A_1\widetilde{\chi}^0_1$) exceeds 10% only for a few points, reaching as high as about 30% for a couple of them. On the other hand, the BR($\widetilde{\chi}^0_2 \to Z\widetilde{\chi}^0_1$), given on the $x$-axis, drops quite sharply with increasing $\lambda$ and can reach as low as about 30%. This is due mainly to the fact that the BR($\widetilde{\chi}^0_2 \to H_2\widetilde{\chi}^0_1$) (not shown here) also rises, much more abruptly than the BR($\widetilde{\chi}^0_2 \to A_1\widetilde{\chi}^0_1$), as $\lambda$ increases. Figure 5(b) shows that the BR($\widetilde{\chi}^0_3 \to A_1\widetilde{\chi}^0_1$) never exceeds 9% while the BR($\widetilde{\chi}^0_3 \to Z\widetilde{\chi}^0_1$) never falls below 50%, implying a relatively weaker dependence on $\lambda$. The heat map in the figure shows that the maximum BR($A_1 \to \mu^+\mu^-$) achievable is 9%. Note that the BR($\widetilde{\chi}^\pm_1 \to W^\pm\widetilde{\chi}^0_1$) is unity for all the points shown in these figures.

We point out here that we also carried out a test scan of the NMSSM with partial universality at the grand unification (GUT) scale. In this model the unified scalar mass parameter, $m_0$, the universal gaugino mass, $m_{1/2}$, the universal Higgs-sfermion trilinear couplings, $a_0$, as well as the paramaters $a_\lambda$ and $a_\kappa$ are input at the GUT scale. The EW scale values of the individual soft scalar and gaugino masses and of all the Higgs trilinear couplings are obtained by the running of these parameters using the renormalization group

[2] Due to the nature of the neutralino mass matrix, given in eq. (2.5), both positive and negative values of the $\widetilde{\chi}^0_3$ mass are possible, although we show here only negative valued solutions. Positivity of $m_{\widetilde{\chi}^0_3}$ can be ensured a priori by a phase transformation.



JHEP07(2015)002

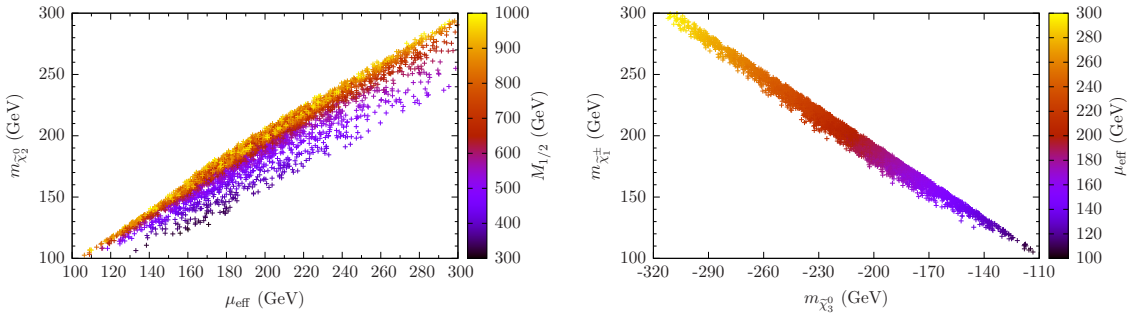


**(a)** **(b)**

**Figure 4.** (a) The $\widetilde{\chi}_2^0$ mass as a function of the parameter $\mu_{\rm eff}$. The color map shows the dependence on $M_{1/2}$. (b) The distribution of the $\widetilde{\chi}_3^0$ and $\widetilde{\chi}_1^\pm$ masses vs. $\mu_{\rm eff}$, shown by the heat map.

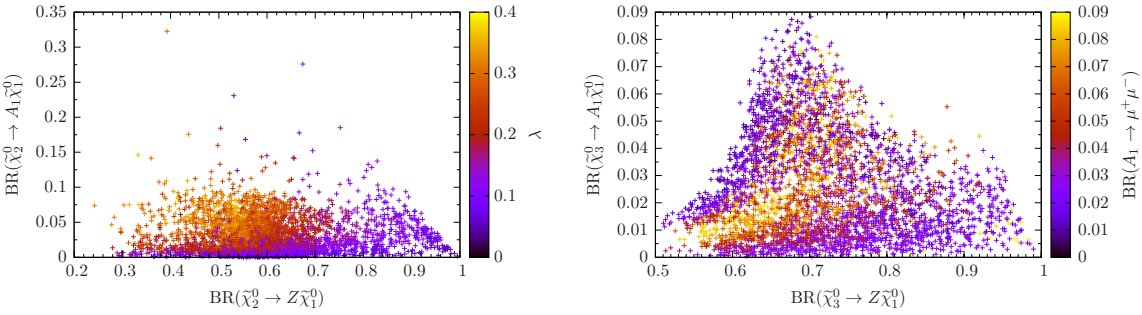


**(a)** **(b)**

**Figure 5.** (a) The BR($\widetilde{\chi}_2^0 \to Z\widetilde{\chi}_1^0$) and the BR($\widetilde{\chi}_2^0 \to A_1\widetilde{\chi}_1^0$) as functions of the parameter $\lambda$. (b) The BR($\widetilde{\chi}_3^0 \to Z\widetilde{\chi}_1^0$) vs. the BR($\widetilde{\chi}_3^0 \to A_1\widetilde{\chi}_1^0$), with the heat map corresponding to the BR($A_1 \to \mu^+\mu^-$).

equations. The other Higgs sector parameters, $\lambda$, $\kappa$, $\mu_{\rm eff}$ and $\tan\beta$ are input at $M_{\rm SUSY}$. But, owing particularly to the GUT scale definition of the parameters $a_\lambda$ and $a_\kappa$, severe fine-tuning is necessary in this model for the scan to find the right combinations of these parameters at $M_{\rm SUSY}$ that yield both $H_2$ and $A_1$ with the desired masses.

As noted above in figure 3(a), $A_\kappa$ at $M_{\rm SUSY}$ is restricted to a narrow range of values, which would imply an even smaller set of its possible values at the GUT scale. Furthermore, the SUSY-preserving parameter $\kappa$ is also very small due to our requirement of $m_{\widetilde{\chi}_1^0} \sim 1.5\,\text{GeV}$, though the approximate PQ symmetry this results in still avoids the cosmological constraints on the PQ axion [76]. Keeping $\mu_{\rm eff}$ around the EW scale, $\kappa$ is typically smaller than $0.01\lambda$. Despite all these limiting conditions, some points with the right masses of the $\widetilde{\chi}_1^0$ and $A_1$ were indeed found. However, they did not cover, for example, the wide range



JHEP07(2015)002

| Selection | SRnoZa | SRnoZb | SRnoZc | SRZa | SRZb | SRZc |
|---|---|---|---|---|---|---|
| $m_{\rm SFOS}$ | $< 60$ | $60 - 81.2$ | $< 81.2$ or $> 101.2$ | $81.2 - 101.2$ | $81.2 - 101.2$ | $81.2 - 101.2$ |
| $\not{E}_T$ | $> 50$ | $> 75$ | $> 75$ | $75 - 120$ | $75 - 120$ | $> 120$ |
| $M_T$ | – | – | $> 110$ | $< 110$ | $> 110$ | $> 110$ |
| $p_{T(\ell_3)}$ | $> 10$ | $> 10$ | $> 30$ | $> 10$ | $> 10$ | $> 10$ |
| SR veto | SRnoZc | SRnoZc | – | – | – | – |

**Table 2.** Selection requirements for the six signal regions defined for the trilepton searches by the ATLAS collaboration. All the dimensionful parameters in rows $2-5$ are in units of GeV.

of the BR($\widetilde{\chi}_2^0 \to A_1\widetilde{\chi}_1^0$) seen in figure 5(a), which stretches beyond 0.1. We therefore opted for the 9-parameter EW-scale NMSSM for this study.

## 4 Very light DM via higgsino decays at the LHC

For our signal-to-background analyses, we selected two benchmark points, BP1 and BP2, out of the good points from the NMSSM parameter space scan. BP1 is chosen such that the BR($\widetilde{\chi}_{2,3}^0 \to Z\widetilde{\chi}_1^0$) is sufficiently large, while BP2 has a relatively enhanced BR($\widetilde{\chi}_{2,3}^0 \to A_1\widetilde{\chi}_1^0$). The parton-level signal and background events for these points were generated with MadGraph5_aMC@NLO [77] and passed to Pythia 6.4 [78] for hadronization.

### 4.1 The trilepton channel

As noted earlier, the ATLAS and CMS experiments have separately performed searches for trileptons ($3\ell$) [61–63] resulting from the $\widetilde{\chi}_{2,3}^0\widetilde{\chi}_1^\pm$ pair production. In the ATLAS $3\ell$ search [61], which is the one we will consider in the following, six signal regions (SRs) are defined in terms of the invariant mass of two same flavor leptons with opposite sign (SFOS), $m_{\rm SFOS}$. These regions also depend on the momentum, $p_{T(\ell_3)}$, of the third lepton, $\ell_3$, that is left after requiring two SFOS leptons to reconstruct $m_{\rm SFOS}$, $\not{E}_T$ and the transverse mass, $M_T = \sqrt{2\,\not{E}_T\,p_{T(\ell_3)}\,(1-\cos\Delta\phi_{\ell_3,\not{E}_T})}$, where $\Delta\phi_{\ell_3,\not{E}_T}$ is the azimuthal angle between $\not{E}_T$ and the $\ell_3$. The signal regions are divided into three '$Z$-enriched' ones, SRZ{a,b,c}, where $m_{\rm SFOS}$ lies within 10 GeV of $m_Z$, and three '$Z$-depleted' ones, SRnoZ{a,b,c}, where $m_{\rm SFOS}$ lies outside this mass window. Table 2 further shows the selection requirements for each of these six regions.

The irreducible backgrounds include di-boson, tri-boson and $t\bar{t}W/Z$ productions, all of which can have three or more leptons and $\not{E}_T$ in the final states. The $ZZ$ and $ZW^\pm$ backgrounds are by far dominant over the $t\bar{t}W/Z$ one [61]. Among the reducible backgrounds are included top quarks produced singly or in pairs, $WW$ and $W$ or $Z$ bosons produced in association with jets or photons. Among these the $t\bar{t}$ background is highly dominant. For each BP, the cross section for the signal process was calculated at next-to-leading order (NLO) using Prospino-v2.1 [79]. We then first generated the event files corresponding to $\sqrt{s} = 8$ TeV for the signal process and passed these to the public package CheckMATE-v1.2.0 [80] for testing against the current LHC limits from the trilepton



JHEP07(2015)002

searches. In CheckMATE the signal regions given in table 2 have been defined and the corresponding backgrounds from the ATLAS experiment implemented. For testing a model point it therefore calculates the signal efficiency for each region, after ATLAS detector simulation with DELPHES 3 [81].

After confirming that the given BP is not excluded by the available data, we proceeded to the future $3\ell$ search at the 14 TeV LHC. We generated the signal event files for $\sqrt{s} =$ 14 TeV and passed these to CheckMATE again. In this way we obtained the signal efficiencies, after multiplying the NLO cross section with an assumed integrated luminosity, $\mathcal{L}$, of 300 fb$^{-1}$ (i.e., design luminosity of the LHC) to get the number of signal events in each signal region.

As for the backgrounds, we only simulated the three dominant ones, $ZZ$, $ZW^{\pm}$ and $tt$, for the 14 TeV LHC. We used MadGraph5 to generate the background events and passed these to CheckMATE to get the cut efficiencies for all the backgrounds in each signal region. After multiplying the NLO cross section [82, 83] and the luminosity, we got the number of background events in each signal region.

### 4.2 Collimated muons from an $A_1$

Due to the smallness of the $A_1$ mass of our interest here, the muons it decays into are highly collinear. In order to isolate such muons, we employ the technique of clustering them together into one object, $\mu_{\rm col}$. This method, similar in concept to the construction of a 'lepton-jet' [84–89], has recently been shown in [90] to be very effective for probing highly mass-degenerate higgsinos.

For using this method, the signal events generated for BP1 and BP2 were passed to Pythia 6.4 for hadronization and subsequently to DELPHES 3 for jet-clustering via the anti-$k_T$ [91] algorithm using FastJet-v3.0.6 [92]. The object $\mu_{\rm col}$ is constructed as follows.

1. Require the transverse momentum, $p_T$, larger than 10 GeV for each muon in the signal. In addition, impose the cut $m_{\mu\bar{\mu}} < 5$ GeV on the invariant mass of the muon pair.

2. Define $I_{\rm sum}$ as the scalar sum of the transverse momenta of all additional charged tracks, each with $p_T > 0.5$ GeV, within a cone centered along the momentum vector of $\mu_{\rm col}$ and satisfying $\Delta R = 0.4$. Impose $I_{\rm sum} < 3$ GeV.

The main backgrounds, containing two collinear muons along with a third lepton and $\not{E}_T$, include $W(\to \ell^{\pm}\nu)\gamma^*$ and $Z(\to \ell^+\ell^-)\gamma^*$, wherein the $\mu_{\rm col}$ comes from the photon, and $Wb\bar{b}$, when one of the $b$-jets produces the $\mu_{\rm col}$. The $Z\gamma^*$ background fakes the signal process when one of the two leptons escape undetected. Note that while the $t\bar{t}$ background mentioned above for the $3\ell$ search is also relevant for this signal process, it becomes negligible here owing to the requirement of the two final state muons being highly collinear. In order to isolate these backgrounds, we implement the following cuts.

1. Since the $A_1$ resulting from the higgsino decay is highly boosted, we expect the $\mu_{\rm col}$ from its subsequent decay to have a large $p_T$. We therefore require $p_{T(\mu_{\rm col})} > 50$ GeV. We also require $p_{T(\ell_3)} > 20$ GeV.



JHEP07(2015)002

2. In order to reduce the background a large $\not{E}_T$ is required, so we add the cut $\not{E}_T > 50\,\text{GeV}$.

3. In the $W\gamma^*$ background the $M_T$ distribution has an end point around the $W$ boson mass, which leads us to impose $M_T > 80\,\text{GeV}$.

4. Our signal would appear as a narrow peak in the $m_{\mu_{\text{col}}}$ distribution. Hence, we impose a narrow cut width, $5 \times \sigma_{A_1}$, where $\sigma_{A_1} = 0.26 + 0.0013 m_{A_1}$, around $m_{A_1}$. This parametrization of $\sigma_{A_1}$ follows the mass resolution study of the $J/\Psi$ resonance in [93]. We also remove the $J/\Psi$ resonance region ($3.0\,\text{GeV} < m_{\mu_{\text{col}}} < 3.2\,\text{GeV}$).

To get a sufficient number of Monte Carlo events in the kinematic regime of our interest, we require $m_{\mu\bar{\mu}} > 1.5\,\text{GeV}$ and $p_{T(\ell_3)} > 10\,\text{GeV}$ at the parton level for the $W\gamma^*$ and $Z\gamma^*$ backgrounds. For the $Wb\bar{b}$ background, we additionally require the $p_T$ of the $b$-jet to be larger than 30 GeV.

## 5 Results and discussion

In table 3 are recorded some specifics of the two BPs used for the signal-to-background analyses. The consistency of each of the $H_2$ signal rates given in the last three rows of the table is to be checked against the experimental quantity $\mu^X \equiv \frac{\sigma(pp\to H_{\text{obs}}\to X)}{\sigma(pp\to h_{\text{SM}}\to X)}$ for each corresponding channel $X$. Note that this comparison assumes that the inclusive $pp$ cross section for $H_2$ production can be approximated by the dominant gluon-fusion production cross section. Note also that, since the $WW$ and $ZZ$ decays of $H_2$ are proportional to the same coupling, NMSSMTools provides a unique value of the signal rates for these two channels, which we denote by $R^{VV}$ in the table. The most recent measurements of $\mu^X$ by the CMS (ATLAS) collaboration(s) read [94–97]

$$\begin{aligned} \mu^{\gamma\gamma} &= 1.13 \pm 0.24\ (1.17 \pm 0.27)\,, \\ \mu^{ZZ(WW)} &= 1.0 \pm 0.29\ (1.09^{+0.23}_{-0.21})\,, \\ \mu^{\tau\tau} &= 0.91 \pm 0.28\ (1.4^{+0.5}_{-0.4})\,. \end{aligned} \tag{5.1}$$

Using each of the two analysis methods described in the previous section we calculated the number of signal events, $S$, and that of background events, $B$, for each BP at the LHC with $\sqrt{s} = 14\,\text{TeV}$ and $\mathcal{L} = 300\ \text{fb}^{-1}$. In table 4 we provide the $S$ and $B$ corresponding to each of the six signal regions in the ATLAS $3\ell$ search. The total signal cross sections obtained are 24.3 fb and 3.93 fb for BP1 and BP2, respectively. In the $Z$-enriched region, $ZW^{\pm}$ production dominates the total background. In the $Z$-depleted region, a comparable contribution is obtained from the $t\bar{t}$ background. One can notice in the table that for both the BPs, the highest sensitivity is obtained in the signal region SRZc.

In the $\mu_{\text{col}}$ channel, the cross sections for the signal and background processes are given in table 5 for the BP1, along with the efficiency of the cuts and the effective cross sections and numbers of events after implementing these cuts. One notices that the $Wb\bar{b}$ is by far the largest background. It, however, gets greatly reduced by the cuts, after which $W\gamma^*$



JHEP07(2015)002

| | BP1 | BP2 |
|---|---|---|
| *Model parameters* | | |
| $M_0$ (GeV) | 1951.1 | 1826.0 |
| $M_{1/2}$ (GeV) | 892.24 | 929.2 |
| $A_0$ (GeV) | 2462.2 | 2626.2 |
| $\mu_{\text{eff}}$ (GeV) | 191.34 | 164.52 |
| $\tan\beta$ | 14.056 | 19.785 |
| $\lambda$ | 0.0814 | 0.3102 |
| $\kappa$ | 0.0002 | 0.0008 |
| $A_\lambda$ (GeV) | 4080.2 | 3596.7 |
| $A_\kappa$ (GeV) | −3.6681 | −6.8466 |
| *Masses* | | |
| $m_{\widetilde{\chi}_1^0}$ (GeV) | 1.0025 | 1.4081 |
| $m_{\widetilde{\chi}_2^0}$ (GeV) | 189.09 | 170.13 |
| $m_{\widetilde{\chi}_3^0}$ (GeV) | −201.67 | −182.27 |
| $m_{\widetilde{\chi}_1^\pm}$ (GeV) | 194.97 | 167.72 |
| $m_{A_1}$ (GeV) | 2.1776 | 2.9856 |
| $m_{H_2}$ (GeV) | 124.12 | 125.79 |
| *Branching ratios* | | |
| $BR(\widetilde{\chi}_2^0 \to Z\widetilde{\chi}_1^0)$ | 0.634 | 0.603 |
| $BR(\widetilde{\chi}_2^0 \to A_1\widetilde{\chi}_1^0)$ | 0.004 | 0.089 |
| $BR(\widetilde{\chi}_3^0 \to Z\widetilde{\chi}_1^0)$ | 0.736 | 0.704 |
| $BR(\widetilde{\chi}_3^0 \to A_1\widetilde{\chi}_1^0)$ | 0.004 | 0.081 |
| $BR(A_1 \to \mu^+\mu^-)$ | 0.039 | 0.087 |
| $H_2$ *signal rates* | | |
| $R^{\gamma\gamma}$ | 0.998 | 0.901 |
| $R^{VV}$ | 0.996 | 0.885 |
| $R^{\tau\tau}$ | 1.003 | 0.847 |

**Table 3.** Properties of the two benchmark points used for the signal-to-background analyses.

JHEP07(2015)002

| Background or signal | SRnoZa | SRnoZb | SRnoZc | SRZa | SRZb | SRZc |
|---|---|---|---|---|---|---|
| $ZZ$ events | 410 | 59 | 10 | 280 | 39 | 12 |
| $ZW^{\pm}$ events | 1391 | 595 | 71 | 6850 | 661 | 189 |
| $t\bar{t}$ events | 1715 | 401 | 62 | 272 | 178 | 19 |
| All background events | 3516 | 1055 | 143 | 7402 | 878 | 220 |
| BP1 signal events | 12 | 37 | 19 | 191 | 134 | 130 |
| BP2 signal events | 20 | 46 | 18 | 270 | 144 | 96 |

**Table 4.** The number of background and signal events at the 14 TeV LHC for $\mathcal{L} = 300\,\text{fb}^{-1}$ in each of the signal regions of the ATLAS $3\ell$ search.

| | BP1 | $W\gamma^*$ | $Z\gamma^*$ | $Wb\bar{b}$ |
|---|---|---|---|---|
| Cross section (fb) | 0.178 | 246.9 | 10.0 | 3770.0 |
| Cut efficiency | 0.123 | $2.15 \times 10^{-4}$ | $6 \times 10^{-5}$ | $1 \times 10^{-6}$ |
| Effective cross section (fb) | 0.022 | 0.053 | 0.0006 | 0.003 |
| No. of events | 6.6 | 15.9 | 0.18 | 0.9 |

**Table 5.** The backgrounds and the signal for the BP1 in the $\mu_{\text{col}}$ search channel at the 14 TeV LHC for $\mathcal{L} = 300\,\text{fb}^{-1}$.

takes over as the most dominant background. The corresponding quantities for the BP2 are listed in table 6. Due to the different masses of the $A_1$ and $\widetilde{\chi}_1^0$ obtained for the two BPs, different sets of cuts need to be implemented for each of them.

We quantify the strengths of the two analyses in terms of $S/B$ for comparing them against each other. This quantity is listed in table 7 for the two BPs in each of the search channel. The $3\ell$ analysis gives a slightly higher $S/B$ for the BP1 compared to that for the BP2. On the other hand, $S/B$ for the BP2 in the $\mu_{\text{col}}$ analysis is considerably larger than the $S/B$ obtained for the BP1 in each of the two analyses. This is due, evidently, to the sizable $\text{BR}(\widetilde{\chi}_2^0 \to A_1\widetilde{\chi}_1^0)$ and $\text{BR}(A_1 \to \mu^+\mu^-)$, as noted in table 3. In addition, the cut efficiency for the signal is much higher while that for the $W\gamma^*$ background is much lower in the case of the BP1.

For a more realistic analysis of the prospects of a signal process though, the statistical and systematic uncertainties in it also need to be taken into account. Hence, for each BP we have also provided in table 7 the statistical significance, given by the approximate formula,

$$\mathcal{Z} \equiv \frac{S}{\sqrt{B + (\varepsilon B)^2}}\,, \tag{5.2}$$

where the systematic uncertainty is given by the fraction $\varepsilon$ of the background. From the ATLAS $3\ell$ search [61], we note that the systematic uncertainty is 21% for the SRZc signal region, where the highest sensitivity is achieved, as seen above. We expect this number not to vary considerably at the 14 TeV LHC and hence use $\varepsilon = 0.21$ in our estimation



JHEP07(2015)002

| | BP2 | $W\gamma^*$ | $Z\gamma^*$ | $Wb\bar{b}$ |
|---|---|---|---|---|
| Cross section (fb) | 3.93 | 246.9 | 10.0 | 3770.0 |
| Cut efficiency | 0.050 | $5.3 \times 10^{-5}$ | $3 \times 10^{-5}$ | $1 \times 10^{-6}$ |
| Effective cross section (fb) | 0.197 | 0.013 | 0.0003 | 0.003 |
| No. of events | 59.1 | 3.9 | 0.09 | 0.9 |

**Table 6.** The backgrounds and the signal for the BP2 in the $\mu_{\rm col}$ search channel at the 14 TeV LHC for $\mathcal{L} = 300\,{\rm fb}^{-1}$.

| Point | $S/B$ in analysis | | $\mathcal{Z}$ $(\sigma)$ in analysis | |
|---|---|---|---|---|
| | $3\ell$ (SRZc region) | $\mu_{\rm col}$ | $3\ell$ (SRZc region) | $\mu_{\rm col}$ |
| BP1 | 0.591 | 0.42 | 2.7 | 1.2 |
| BP2 | 0.436 | 15 | 2.0 | 27 |

**Table 7.** Results in the two analyses methods for the benchmark points.

of $\mathcal{Z}$ for the $3\ell$ channel. For the $W + \mu_{\rm col} + \not{E}_T$ channel, since there is no experimental analysis available, the systematic uncertainty has to be estimated roughly. There are two major sources of this uncertainty: the reconstruction of the $\mu_{\rm col}$, in which case it is around 5% [51], and that of the $\ell_3$, where it is less than 2% [98]. As a conservative estimate, which also allows a direct comparison between the $3\ell$ channel and this channel, we set $\varepsilon = 0.21$ here also. This results in $\mathcal{Z} = 27\,\sigma$ in this channel for the BP2, as seen in table 7, which is much higher than the estimated $\mathcal{Z}$ for the same point in the $3\ell$ channel.

There is, however, a caveat here. As noted from table 6, $B$ for the BP2 is much smaller than $S$, resulting in a large $S/B$. In such a case, the approximate expression for $\mathcal{Z}$, which assumes $S \ll B$, is in principle not valid [99]. While, for a consistent treatment of the systematic uncertainties between the two search channels, we retain this approximate expression for the $\mu_{\rm col}$ channel also, we emphasize that the given $S/B$ values be considered a much more accurate estimate of the strength of each channel at the 14 TeV LHC.

## 6 Conclusions

In this article we have discussed an $\mathcal{O}(1)$ GeV neutralino DM in the NMSSM and its detectability at the LHC. Despite being very light, such a singlino-like DM can generate thermal relic abundance of the universe consistent with the PLANCK measurement, owing to the existence also of a singlet-like pseudoscalar, $A_1$, with a mass around twice the DM mass. A very light DM giving the correct relic abundance is impossible to obtain in the MSSM, and thus its detection will provide a clear indication of physics beyond minimal SUSY. We have noted that the current direct and indirect detection facilities have very poor detection prospects for such a light DM with and hence its dedicated searches at the LHC can prove very crucial. We have therefore studied in depth the prospects for its observation at the 14 TeV LHC.



JHEP07(2015)002

By performing a through scan of the NMSSM parameter space, chosen taking into account the analytical structure of the neutralino mass matrix, we found a variety of its configurations where an $\mathcal{O}(1)$ GeV DM can be obtained. We then carried out detector-level analyses of two of the main production modes of such a DM. In both these modes, the DM is produced in the decays of a higgsino-like heavier neutralino, $\widetilde{\chi}^0_{2/3}$, which itself is produced in a pair with the lightest chargino. The $\widetilde{\chi}^0_{2/3}$ then decays into either $Z + \mathrm{DM}$ or $A_1 + \mathrm{DM}$. The former channel, combined with the chargino decay, results in a trilepton $+ \not{E}_T$ final state, for which dedicated searches are already being performed by the CMS and ATLAS collaborations. In the latter channel the final state comprises of a pair of muons and a third lepton along with the DM.

In the $\widetilde{\chi}^0_{2,3} \to \mathrm{DM} + A_1$ channel, the two muons that the very light $A_1$ decays into are highly collinear. Therefore, this channel can not be probed using the usual muon identification criteria. For this reason, we have adopted the technique of grouping the two muons together into a single jet-like object by applying certain unconventional rigorous cuts. By implementing this method on two benchmark points from our scan, we have found that this channel can have a signal strength comparable to that of the trilepton channel at the 14 TeV LHC with $\mathcal{L} = 300$ fb$^{-1}$. In fact, for one of the two points, wherein the $\mathrm{BR}(\widetilde{\chi}^0_{2,3} \to \mathrm{DM} + A_1)$ is significant and the $\mathrm{BR}(A_1 \to \mu^+\mu^-)$ is maximal, the obtained $S/B$ for this cannel is much larger than that for the trilepton channel. We thus emphasize that dedicated searches in this channel may prove very crucial for the discovery of a very light SUSY DM within a few years of the current LHC run.

## Acknowledgments

C. Han is thankful to Peiwen Wu for useful discussions. This work is supported by the Korea Ministry of Science, ICT and Future Planning, Gyeongsangbuk-Do and Pohang City for Independent Junior Research Groups at the Asia Pacific Center for Theoretical Physics. MP is also supported by World Premier International Research Center Initiative (WPI Initiative), MEXT, Japan.



## References

[1] CMS collaboration, *Observation of a new boson at a mass of* 125 *GeV with the CMS experiment at the LHC*, *Phys. Lett.* **B 716** (2012) 30 [arXiv:1207.7235] [INSPIRE].

[2] ATLAS collaboration, *Observation of a new particle in the search for the standard model Higgs boson with the ATLAS detector at the LHC*, *Phys. Lett.* **B 716** (2012) 1 [arXiv:1207.7214] [INSPIRE].

[3] WMAP collaboration, G. Hinshaw et al., *Nine-year Wilkinson Microwave Anisotropy Probe (WMAP) observations: cosmological parameter results*, *Astrophys. J. Suppl.* **208** (2013) 19 [arXiv:1212.5226] [INSPIRE].



JHEP07(2015)002

[4] Planck collaboration, P.A.R. Ade et al., *Planck* 2015 *results. XIII. Cosmological parameters*, arXiv:1502.01589 [INSPIRE].

[5] A. Fowlie, K. Kowalska, L. Roszkowski, E.M. Sessolo and Y.-L.S. Tsai, *Dark matter and collider signatures of the MSSM*, *Phys. Rev.* **D 88** (2013) 055012 [arXiv:1306.1567] [INSPIRE].

[6] P. Bergeron and S. Profumo, *IceCube, DeepCore, PINGU and the indirect search for supersymmetric dark matter*, *JCAP* **01** (2014) 026 [arXiv:1312.4445] [INSPIRE].

[7] P. Fayet, *Supergauge invariant extension of the Higgs mechanism and a model for the electron and its neutrino*, *Nucl. Phys.* **B 90** (1975) 104 [INSPIRE].

[8] J.R. Ellis, J.F. Gunion, H.E. Haber, L. Roszkowski and F. Zwirner, *Higgs bosons in a nonminimal supersymmetric model*, *Phys. Rev.* **D 39** (1989) 844 [INSPIRE].

[9] L. Durand and J.L. Lopez, *Upper bounds on Higgs and top quark masses in the flipped* $SU(5) \times U(1)$ *superstring model*, *Phys. Lett.* **B 217** (1989) 463 [INSPIRE].

[10] M. Drees, *Supersymmetric models with extended Higgs sector*, *Int. J. Mod. Phys.* **A 4** (1989) 3635 [INSPIRE].

[11] U. Ellwanger, *A Higgs boson near* 125 *GeV with enhanced di-photon signal in the NMSSM*, *JHEP* **03** (2012) 044 [arXiv:1112.3548] [INSPIRE].

[12] S.F. King, M. Muhlleitner and R. Nevzorov, *NMSSM Higgs benchmarks near* 125 *GeV*, *Nucl. Phys.* **B 860** (2012) 207 [arXiv:1201.2671] [INSPIRE].

[13] U. Ellwanger and C. Hugonie, *Higgs bosons near* 125 *GeV in the NMSSM with constraints at the GUT scale*, *Adv. High Energy Phys.* **2012** (2012) 625389 [arXiv:1203.5048] [INSPIRE].

[14] T. Gherghetta, B. von Harling, A.D. Medina and M.A. Schmidt, *The scale-invariant NMSSM and the* 126 *GeV Higgs boson*, *JHEP* **02** (2013) 032 [arXiv:1212.5243] [INSPIRE].

[15] J.-J. Cao, Z.-X. Heng, J.M. Yang, Y.-M. Zhang and J.-Y. Zhu, *A SM-like Higgs near* 125 *GeV in low energy SUSY: a comparative study for MSSM and NMSSM*, *JHEP* **03** (2012) 086 [arXiv:1202.5821] [INSPIRE].

[16] J.F. Gunion, Y. Jiang and S. Kraml, *Could two NMSSM Higgs bosons be present near* 125 *GeV?*, *Phys. Rev.* **D 86** (2012) 071702 [arXiv:1207.1545] [INSPIRE].

[17] J.F. Gunion, Y. Jiang and S. Kraml, *Diagnosing degenerate Higgs bosons at* 125 *GeV*, *Phys. Rev. Lett.* **110** (2013) 051801 [arXiv:1208.1817] [INSPIRE].

[18] S.F. King, M. Mühlleitner, R. Nevzorov and K. Walz, *Natural NMSSM Higgs bosons*, *Nucl. Phys.* **B 870** (2013) 323 [arXiv:1211.5074] [INSPIRE].

[19] M. Carena, N.R. Shah and C.E.M. Wagner, *Light dark matter and the electroweak phase transition in the NMSSM*, *Phys. Rev.* **D 85** (2012) 036003 [arXiv:1110.4378] [INSPIRE].

[20] X.-J. Bi, L. Bian, W. Huang, J. Shu and P.-F. Yin, *The interpretation for galactic center excess and electroweak phase transition in the NMSSM*, arXiv:1503.03749 [INSPIRE].

[21] D. Hooper and L. Goodenough, *Dark matter annihilation in the galactic center as seen by the Fermi gamma ray space telescope*, *Phys. Lett.* **B 697** (2011) 412 [arXiv:1010.2752] [INSPIRE].

[22] D. Hooper and T. Linden, *On the origin of the gamma rays from the galactic center*, *Phys. Rev.* **D 84** (2011) 123005 [arXiv:1110.0006] [INSPIRE].

JHEP07(2015)002

[23] C. Cheung, M. Papucci, D. Sanford, N.R. Shah and K.M. Zurek, *NMSSM interpretation of the galactic center excess*, *Phys. Rev.* **D 90** (2014) 075011 [arXiv:1406.6372] [INSPIRE].

[24] J. Cao, L. Shang, P. Wu, J.M. Yang and Y. Zhang, *Supersymmetry explanation of the Fermi galactic center excess and its test at LHC run II*, *Phys. Rev.* **D 91** (2015) 055005 [arXiv:1410.3239] [INSPIRE].

[25] L. Feng, S. Profumo and L. Ubaldi, *Closing in on singlet scalar dark matter: LUX, invisible Higgs decays and gamma-ray lines*, *JHEP* **03** (2015) 045 [arXiv:1412.1105] [INSPIRE].

[26] J. Kozaczuk and S. Profumo, *Light NMSSM neutralino dark matter in the wake of CDMS II and a* 126 *GeV Higgs boson*, *Phys. Rev.* **D 89** (2014) 095012 [arXiv:1308.5705] [INSPIRE].

[27] J. Cao, C. Han, L. Wu, P. Wu and J.M. Yang, *A light SUSY dark matter after CDMS-II, LUX and LHC Higgs data*, *JHEP* **05** (2014) 056 [arXiv:1311.0678] [INSPIRE].

[28] CDMS collaboration, R. Agnese et al., *Silicon detector dark matter results from the final exposure of CDMS II*, *Phys. Rev. Lett.* **111** (2013) 251301 [arXiv:1304.4279] [INSPIRE].

[29] DAMA, LIBRA collaboration, R. Bernabei et al., *New results from DAMA/LIBRA*, *Eur. Phys. J.* **C 67** (2010) 39 [arXiv:1002.1028] [INSPIRE].

[30] CoGeNT collaboration, C.E. Aalseth et al., *Results from a search for light-mass dark matter with a P-type point contact germanium detector*, *Phys. Rev. Lett.* **106** (2011) 131301 [arXiv:1002.4703] [INSPIRE].

[31] CoGeNT collaboration, C.E. Aalseth et al., *Search for an annual modulation in a P-type point contact germanium dark matter detector*, *Phys. Rev. Lett.* **107** (2011) 141301 [arXiv:1106.0650] [INSPIRE].

[32] G. Angloher et al., *Results from* 730 *kg days of the CRESST-II dark matter search*, *Eur. Phys. J.* **C 72** (2012) 1971 [arXiv:1109.0702] [INSPIRE].

[33] XENON100 collaboration, E. Aprile et al., *Dark matter results from* 225 *live days of XENON*100 *data*, *Phys. Rev. Lett.* **109** (2012) 181301 [arXiv:1207.5988] [INSPIRE].

[34] LUX collaboration, D.S. Akerib et al., *First results from the LUX dark matter experiment at the Sanford Underground Research Facility*, *Phys. Rev. Lett.* **112** (2014) 091303 [arXiv:1310.8214] [INSPIRE].

[35] P. Draper, T. Liu, C.E.M. Wagner, L.-T. Wang and H. Zhang, *Dark light Higgs*, *Phys. Rev. Lett.* **106** (2011) 121805 [arXiv:1009.3963] [INSPIRE].

[36] R. Enberg, S. Munir, C.P. d.l. Heros and D. Werder, *Prospects for higgsino-singlino dark matter detection at IceCube and PINGU*, arXiv:1506.05714 [INSPIRE].

[37] D. Das, U. Ellwanger and A.M. Teixeira, *Modified signals for supersymmetry in the NMSSM with a singlino-like LSP*, *JHEP* **04** (2012) 067 [arXiv:1202.5244] [INSPIRE].

[38] U. Ellwanger, *Testing the higgsino-singlino sector of the NMSSM with trileptons at the LHC*, *JHEP* **11** (2013) 108 [arXiv:1309.1665] [INSPIRE].

[39] J.S. Kim and T.S. Ray, *The higgsino-singlino world at the Large Hadron Collider*, *Eur. Phys. J.* **C 75** (2015) 40 [arXiv:1405.3700] [INSPIRE].

[40] C. Han, *Probing light bino and higgsinos at the LHC*, arXiv:1409.7000 [INSPIRE].

[41] B. Dutta, Y. Gao and B. Shakya, *Light higgsino decays as a probe of the NMSSM*, *Phys. Rev.* **D 91** (2015) 035016 [arXiv:1412.2774] [INSPIRE].

JHEP07(2015)002

[42] D.G. Cerdeño, P. Ghosh, C.B. Park and M. Peiró, *Collider signatures of a light NMSSM pseudoscalar in neutralino decays in the light of LHC results*, *JHEP* **02** (2014) 048 [arXiv:1307.7601] [INSPIRE].

[43] U. Ellwanger, J.F. Gunion, C. Hugonie and S. Moretti, *Towards a no lose theorem for NMSSM Higgs discovery at the LHC*, hep-ph/0305109 [INSPIRE].

[44] J.R. Forshaw, J.F. Gunion, L. Hodgkinson, A. Papaefstathiou and A.D. Pilkington, *Reinstating the 'no-lose' theorem for NMSSM Higgs discovery at the LHC*, *JHEP* **04** (2008) 090 [arXiv:0712.3510] [INSPIRE].

[45] M.M. Almarashi and S. Moretti, *Low mass Higgs signals at the LHC in the next-to-minimal supersymmetric standard model*, *Eur. Phys. J.* **C 71** (2011) 1618 [arXiv:1011.6547] [INSPIRE].

[46] M.M. Almarashi and S. Moretti, *Muon signals of very light CP-odd Higgs states of the NMSSM at the LHC*, *Phys. Rev.* **D 83** (2011) 035023 [arXiv:1101.1137] [INSPIRE].

[47] M.M. Almarashi and S. Moretti, *LHC signals of a heavy CP-even Higgs boson in the NMSSM via decays into a Z and a light CP-odd Higgs state*, *Phys. Rev.* **D 85** (2012) 017701 [arXiv:1109.1735] [INSPIRE].

[48] U. Ellwanger, *Higgs pair production in the NMSSM at the LHC*, *JHEP* **08** (2013) 077 [arXiv:1306.5541] [INSPIRE].

[49] J. Cao, F. Ding, C. Han, J.M. Yang and J. Zhu, *A light Higgs scalar in the NMSSM confronted with the latest LHC Higgs data*, *JHEP* **11** (2013) 018 [arXiv:1309.4939] [INSPIRE].

[50] CMS collaboration, *Search for a light pseudoscalar Higgs boson in the dimuon decay channel in pp collisions at* $\sqrt{s} = 7$ *TeV*, *Phys. Rev. Lett.* **109** (2012) 121801 [arXiv:1206.6326] [INSPIRE].

[51] CMS collaboration, *Search for a non-standard-model Higgs boson decaying to a pair of new light bosons in four-muon final states*, *Phys. Lett.* **B 726** (2013) 564 [arXiv:1210.7619] [INSPIRE].

[52] N.-E. Bomark, S. Moretti, S. Munir and L. Roszkowski, *A light NMSSM pseudoscalar Higgs boson at the LHC redux*, *JHEP* **02** (2015) 044 [arXiv:1409.8393] [INSPIRE].

[53] D. Curtin, R. Essig and Y.-M. Zhong, *Uncovering light scalars with exotic Higgs decays to* $b\bar{b}\mu^+\mu^-$, *JHEP* **06** (2015) 025 [arXiv:1412.4779] [INSPIRE].

[54] N.-E. Bomark, S. Moretti and L. Roszkowski, *Detection prospects of light NMSSM Higgs pseudoscalar via cascades of heavier scalars from vector boson fusion and Higgs-strahlung*, arXiv:1503.04228 [INSPIRE].

[55] U. Ellwanger, C. Hugonie and A.M. Teixeira, *The next-to-minimal supersymmetric standard model*, *Phys. Rept.* **496** (2010) 1 [arXiv:0910.1785] [INSPIRE].

[56] M. Maniatis, *The next-to-minimal supersymmetric extension of the standard model reviewed*, *Int. J. Mod. Phys.* **A 25** (2010) 3505 [arXiv:0906.0777] [INSPIRE].

[57] R.D. Peccei and H.R. Quinn, *CP conservation in the presence of instantons*, *Phys. Rev. Lett.* **38** (1977) 1440 [INSPIRE].

[58] R.D. Peccei and H.R. Quinn, *Constraints imposed by CP conservation in the presence of instantons*, *Phys. Rev.* **D 16** (1977) 1791 [INSPIRE].

JHEP07(2015)002

[59] D.J. Miller, R. Nevzorov and P.M. Zerwas, *The Higgs sector of the next-to-minimal supersymmetric standard model*, *Nucl. Phys.* **B 681** (2004) 3 [hep-ph/0304049] [INSPIRE].

[60] T. Han, Z. Liu and S. Su, *Light neutralino dark matter: direct/indirect detection and collider searches*, *JHEP* **08** (2014) 093 [arXiv:1406.1181] [INSPIRE].

[61] ATLAS collaboration, *Search for direct production of charginos and neutralinos in events with three leptons and missing transverse momentum in* $21\,\text{fb}^{-1}$ *of pp collisions at* $\sqrt{s} = 8$ *TeV with the ATLAS detector*, ATLAS-CONF-2013-035, CERN, Geneva Switzerland (2013).

[62] ATLAS collaboration, *Search for direct production of charginos and neutralinos in events with three leptons and missing transverse momentum in* $\sqrt{s} = 8$ *TeV pp collisions with the ATLAS detector*, *JHEP* **04** (2014) 169 [arXiv:1402.7029] [INSPIRE].

[63] CMS collaboration, *Searches for electroweak production of charginos, neutralinos and sleptons decaying to leptons and W, Z and Higgs bosons in pp collisions at* 8 *TeV*, *Eur. Phys. J.* **C 74** (2014) 3036 [arXiv:1405.7570] [INSPIRE].

[64] F. Feroz, M.P. Hobson and M. Bridges, *MultiNest: an efficient and robust Bayesian inference tool for cosmology and particle physics*, *Mon. Not. Roy. Astron. Soc.* **398** (2009) 1601 [arXiv:0809.3437] [INSPIRE].

[65] U. Ellwanger, J.F. Gunion and C. Hugonie, *NMHDECAY: a fortran code for the Higgs masses, couplings and decay widths in the NMSSM*, *JHEP* **02** (2005) 066 [hep-ph/0406215] [INSPIRE].

[66] U. Ellwanger and C. Hugonie, *NMHDECAY* 2.0*: an updated program for sparticle masses, Higgs masses, couplings and decay widths in the NMSSM*, *Comput. Phys. Commun.* **175** (2006) 290 [hep-ph/0508022] [INSPIRE].

[67] D. Das, U. Ellwanger and A.M. Teixeira, *NMSDECAY: a fortran code for supersymmetric particle decays in the next-to-minimal supersymmetric standard model*, *Comput. Phys. Commun.* **183** (2012) 774 [arXiv:1106.5633] [INSPIRE].

[68] *NMSSMTools webpage*, http:/http://www.th.u-psud.fr/NMHDECAY/nmssmtools.html.

[69] M.J. Dolan, C. McCabe, F. Kahlhoefer and K. Schmidt-Hoberg, *A taste of dark matter: flavour constraints on pseudoscalar mediators*, *JHEP* **03** (2015) 171 [arXiv:1412.5174] [INSPIRE].

[70] A. Arbey and F. Mahmoudi, *SuperIso relic: a program for calculating relic density and flavor physics observables in supersymmetry*, *Comput. Phys. Commun.* **181** (2010) 1277 [arXiv:0906.0369] [INSPIRE].

[71] G. Bélanger, F. Boudjema, A. Pukhov and A. Semenov, *MicrOMEGAs*4.1*: two dark matter candidates*, *Comput. Phys. Commun.* **192** (2015) 322 [arXiv:1407.6129] [INSPIRE].

[72] P. Bechtle, O. Brein, S. Heinemeyer, G. Weiglein and K.E. Williams, *HiggsBounds: confronting arbitrary Higgs sectors with exclusion bounds from LEP and the Tevatron*, *Comput. Phys. Commun.* **181** (2010) 138 [arXiv:0811.4169] [INSPIRE].

[73] P. Bechtle, O. Brein, S. Heinemeyer, G. Weiglein and K.E. Williams, *HiggsBounds* 2.0.0*: confronting neutral and charged Higgs sector predictions with exclusion bounds from LEP and the Tevatron*, *Comput. Phys. Commun.* **182** (2011) 2605 [arXiv:1102.1898] [INSPIRE].

JHEP07(2015)002

[74] P. Bechtle et al., *Recent developments in HiggsBounds and a preview of HiggsSignals*, PoS(CHARGED 2012)024 [arXiv:1301.2345] [INSPIRE].

[75] P. Bechtle et al., *HiggsBounds-4: improved tests of extended Higgs sectors against exclusion bounds from LEP, the Tevatron and the LHC*, *Eur. Phys. J.* **C 74** (2014) 2693 [arXiv:1311.0055] [INSPIRE].

[76] O. Lebedev and S. Ramos-Sanchez, *The NMSSM and string theory*, *Phys. Lett.* **B 684** (2010) 48 [arXiv:0912.0477] [INSPIRE].

[77] J. Alwall et al., *The automated computation of tree-level and next-to-leading order differential cross sections and their matching to parton shower simulations*, *JHEP* **07** (2014) 079 [arXiv:1405.0301] [INSPIRE].

[78] T. Sjöstrand, S. Mrenna and P.Z. Skands, *PYTHIA* 6.4 *physics and manual*, *JHEP* **05** (2006) 026 [hep-ph/0603175] [INSPIRE].

[79] W. Beenakker, M. Krämer, T. Plehn, M. Spira and P.M. Zerwas, *Stop production at hadron colliders*, *Nucl. Phys.* **B 515** (1998) 3 [hep-ph/9710451] [INSPIRE].

[80] M. Drees, H. Dreiner, D. Schmeier, J. Tattersall and J.S. Kim, *CheckMATE: confronting your favourite new physics model with LHC data*, *Comput. Phys. Commun.* **187** (2014) 227 [arXiv:1312.2591] [INSPIRE].

[81] DELPHES 3 collaboration, J. de Favereau et al., *DELPHES* 3*, a modular framework for fast simulation of a generic collider experiment*, *JHEP* **02** (2014) 057 [arXiv:1307.6346] [INSPIRE].

[82] J.M. Campbell, R.K. Ellis and C. Williams, *Vector boson pair production at the LHC*, *JHEP* **07** (2011) 018 [arXiv:1105.0020] [INSPIRE].

[83] R. Bonciani, S. Catani, M.L. Mangano and P. Nason, *NLL resummation of the heavy quark hadroproduction cross-section*, *Nucl. Phys.* **B 529** (1998) 424 [hep-ph/9801375] [INSPIRE].

[84] N. Arkani-Hamed and N. Weiner, *LHC signals for a superunified theory of dark matter*, *JHEP* **12** (2008) 104 [arXiv:0810.0714] [INSPIRE].

[85] N. Arkani-Hamed, D.P. Finkbeiner, T.R. Slatyer and N. Weiner, *A theory of dark matter*, *Phys. Rev.* **D 79** (2009) 015014 [arXiv:0810.0713] [INSPIRE].

[86] M. Baumgart, C. Cheung, J.T. Ruderman, L.-T. Wang and I. Yavin, *Non-Abelian dark sectors and their collider signatures*, *JHEP* **04** (2009) 014 [arXiv:0901.0283] [INSPIRE].

[87] A. Katz and R. Sundrum, *Breaking the dark force*, *JHEP* **06** (2009) 003 [arXiv:0902.3271] [INSPIRE].

[88] C. Cheung, J.T. Ruderman, L.-T. Wang and I. Yavin, *Lepton jets in (supersymmetric) electroweak processes*, *JHEP* **04** (2010) 116 [arXiv:0909.0290] [INSPIRE].

[89] A. Falkowski, J.T. Ruderman, T. Volansky and J. Zupan, *Hidden Higgs decaying to lepton jets*, *JHEP* **05** (2010) 077 [arXiv:1002.2952] [INSPIRE].

[90] C. Han, D. Kim, S. Munir and M. Park, *Accessing the core of naturalness, nearly degenerate higgsinos, at the LHC*, *JHEP* **04** (2015) 132 [arXiv:1502.03734] [INSPIRE].

[91] M. Cacciari, G.P. Salam and G. Soyez, *The anti-$k_t$ jet clustering algorithm*, *JHEP* **04** (2008) 063 [arXiv:0802.1189] [INSPIRE].

[92] M. Cacciari, G.P. Salam and G. Soyez, *FastJet user manual*, *Eur. Phys. J.* **C 72** (2012) 1896 [arXiv:1111.6097] [INSPIRE].



JHEP07(2015)002

[93] CMS collaboration, *Search for light resonances decaying into pairs of muons as a signal of new physics*, *JHEP* **07** (2011) 098 [arXiv:1106.2375] [INSPIRE].

[94] CMS collaboration, *Precise determination of the mass of the Higgs boson and tests of compatibility of its couplings with the standard model predictions using proton collisions at* 7 *and* 8 TeV, *Eur. Phys. J.* **C 75** (2015) 212 [arXiv:1412.8662] [INSPIRE].

[95] ATLAS collaboration, *Measurement of Higgs boson production in the diphoton decay channel in pp collisions at center-of-mass energies of* 7 *and* 8 *TeV with the ATLAS detector*, *Phys. Rev.* **D 90** (2014) 112015 [arXiv:1408.7084] [INSPIRE].

[96] ATLAS collaboration, *Observation and measurement of Higgs boson decays to $WW^*$ with the ATLAS detector*, arXiv:1412.2641 [INSPIRE].

[97] ATLAS collaboration, *Updated coupling measurements of the Higgs boson with the ATLAS detector using up to* $25\,\text{fb}^{-1}$ *of proton-proton collision data*, ATLAS-CONF-2014-009, CERN, Geneva Switzerland (2014).

[98] ATLAS collaboration, *Measurements of $W\gamma$ and $Z\gamma$ production in pp collisions at $\sqrt{s} = 7$ TeV with the ATLAS detector at the LHC*, *Phys. Rev.* **D 87** (2013) 112003 [arXiv:1302.1283] [INSPIRE].

[99] G. Cowan, K. Cranmer, E. Gross and O. Vitells, *Asymptotic formulae for likelihood-based tests of new physics*, *Eur. Phys. J.* **C 71** (2011) 1554 [arXiv:1007.1727] [INSPIRE].

JHEP07(2015)002